Journal of NeuroVirology, 10: 233–243, 2004

ISSN: 1355-0284 print / 1538-2443 online
DOI: 10.1080/13550280490463514

Taylor & Francis
Taylor & Francis Group

In the absence of glycoprotein I (gI), gE determines bovine herpesvirus type 5 neuroinvasiveness and neurovirulence

A Al-Mubarak and SI Chowdhury

Department of Diagnostic Medicine/Pathobiology, College of Veterinary Medicine, Kansas State University, Manhattan, Kansas, USA

Bovine herpesvirus type 5 (BHV-5) is an alphaherpesvirus that causes fatal encephalitis in calves. Envelope glycoproteins E (gE) and gI of alphaherpesviruses are important for the pathogenesis *in vivo*. Previously the authors determined that BHV-5 gE is important for BHV-5 neurovirulence. To determine the role of gI in BHV-5 neurovirulence, the authors have constructed gI-deleted and gI-revertant BHV-5 and analyzed their neuropathogenic properties in a rabbit seizure model. Following intranasal infection, 40% of the rabbits infected with the gI-deleted virus showed severe neurological signs. gI-deleted BHV-5 invaded all the central nervous system (CNS) structures invaded by the gI-revertant BHV-5; however, the number of neurons infected by the gI-deleted virus was similar or slightly reduced (two to four fold). Thus, the gI-deleted virus retained significant neurovirulence and/or neuroinvasive properties when compared with the gE-deleted BHV-5. Pulse-chase analysis revealed that the gE of gI-deleted virus was processed to a larger and a diffused 94- to 100-kDa protein (instead of 94 kDa). The 94- to 100-kDa protein was processed in the Golgi with delayed kinetics but it was endoglycosidase H (EndoH) resistant. In cells infected with gI-deleted virus, there was a reduction in cell-surface gE expression compared to wild-type, which correlated to reduced amount of gE processed in the Golgi. The authors believe that in the absence of gI, BHV-5 gE is sufficient for BHV-5 neurovirulence. *Journal of NeuroVirology* (2004) **10,** 233–243.

Keywords: BHV-5; deletion-effect; glycoprotein E; glycoprotein I; neuropathogenesis; neurovirulence

Introduction

Bovine herpesvirus type 5 (BHV-5) is a neurovirulent alphaherpesvirus that causes fatal encephalitis in calves (Belknap *et al*, 1994; D'Offay *et al*, 1993). Bovine herpesvirus type 1 (BHV-1) is associated with abortions, respiratory infections (subtype 1.1), and genital infections (subtype 1.2) in cattle (Wyler *et al*, 1989), but does not cause encephalitis (Belknap *et al*, 1994). Both BHV-1 and BHV-5 are neurotropic viruses and they establish latency in the trigeminal ganglion (TG) following intranasal and conjunctival inoculation (Ashbaugh *et al*, 1997; Rock *et al*, 1986). In a rabbit seizure model, BHV-1.1 and BHV-5 infections are distinguished by their differential neuropathogenesis (Chowdhury *et al*, 1997). When inoculated intranasally, BHV-5 invades the brain via the olfactory pathway and produces acute neurological signs that are comparable to those seen in calves; however, in BHV-1–inoculated rabbits, the virus does not invade the central nervous system (CNS), and no neurological signs develop (Lee *et al*, 1999).

The glycoprotein E and I (gE/gI) homologues in alphaherpesviruses, including BHV-5, form a noncovalently linked hetero-oligomer complex that is

Address correspondence to S. I. Chowdhury, Department of Diagnostic Medicine/Pathobiology, College of Veterinary Medicine, Kansas State University, Manhattan, KS 66506, USA. E-mail: Chowdh@vet.k-state.edu

The authors thank Dr. Lynn Enquist, Princeton University, for the rabbit anti–BHV-1 gE- and gI-specific antibodies and Rebhi Bsharat for statistical analysis. This work was supported by USDA grants 00-02103 to S. I. Chowdhury. Published as contribution 03-238-J, Kansas Agricultural Experiment Station.

Received 16 December 2003; revised 19 February 2004; accepted 24 February 2004.

required for gE and gI maturation. Together, they form a functional unit that serves as immunoglobulin G Fc receptor (Johnson and Feenstra, 1987; Johnson *et al*, 1988; Litwin *et al*, 1992), and is required for cell to cell spread *in vitro* (Dingwell and Johnson, 1998; Dingwell *et al*, 1995) and neurovirulence *in vivo* (Enquist *et al*, 1999). In pseudorabies virus (PRV) and herpes simplex virus type 1 (HSV-1), gE- or gI-null mutants have significantly reduced neurovirulence and their ability to infect second- and third-order neurons after nasopharyngeal and ocular infection is significantly reduced (Card *et al*, 1992; Card and Enquist, 1995; Dingwell *et al*, 1995; Husak *et al*, 2000). In PRV, in addition to gE and gI, Us9-null mutants have significantly reduced neurovirulence in the rat eye model (Brideau *et al*, 2000; Card *et al*, 1992; Kritas *et al*, 1994, 1995; Mulder *et al*, 1994). In a rabbit seizure model, Us9-deleted BHV-5 infects the olfactory receptor neurons (first-order) but failed to travel anterogradely to the bulb after intranasal inoculation (Chowdhury *et al*, 2002), and gE-deleted BHV-5 infects the olfactory receptor neurons but have restricted anterograde transport to the bulb (second-order neurons) and have severely reduced ability to infect third-order neurons (Chowdhury *et al*, 2000). The role of gI in BHV-5 neuropathogenesis has not yet been determined.

In this study, we investigated the role of gI in BHV-5 neuropathogenesis. We determined the nucleotide sequence of the BHV-5 gI open reading frame (ORF) and compared it with the published coding sequence for the gI ORFs of a Brazilian BHV-5 strain (Delhon *et al*, 2003) and BHV-1 (Leung-Tack *et al*, 1994). We generated gI-deleted BHV-5 and analyzed its neuropathogenicity in a rabbit seizure model. Further, the processing and surface expression of gE in the gI-deleted virus was analyzed.

Results

Analysis of BHV-5 gI ORF and comparison of predicted amino acid sequence of BHV-5 and BHV-1 gI gene

The BHV-5 gI ORF is 387 residues in length, whereas predicted BHV-1 gI ORF contains 382 amino acids. Alignment of the predicted amino acid sequence of the BHV-5 gI ORF with the corresponding sequence of BHV-1.1 showed 80% identity and 82% similarity (Figure 1). The sequence analysis show that the BHV-5 gI has all the characteristics of class I membrane protein. Residues 1 to 18 form a signal sequence with a potential consensus cleavage site (Figure 1) and the residues 302 to 323 form a potential transmembrane domain (Figure 1).

The alignment showed that 12 cysteine residues (one cysteine residue present in the putative signal sequence will be cleaved off and has not been counted) are conserved between the two gI sequences. Four cysteine residues are present in the

Figure 1 Comparison of the predicted amino acid sequences of the BHV-5 gI with the predicted amino acid sequence of BHV-1 gI. The predicted amino acid sequence of BHV-1 and BHV-5 gIs were aligned by using the GCG Gap program. Thirteen conserved cysteine residues are marked by boxes. *N*-linked glycosylation sites are underlined and potential *O*-linked glycosylation sites are indicated (*). The presumptive signal sequences and transmembrane anchor sequences are shown by broken boxes, respectively.

extracellular domain, two in the transmembrane domain, and the rest are in the cytoplasmic domain (Figure 1). A dileucine motif within the cytoplasmic domain is conserved in both the sequences. The BHV-5 gI has two potential N-linked glycosylation sites (residues N_{68} to V_{71} and N_{274} to S_{277}) and 12 potential *O*-linked glycosylation sites (Figure 1). In comparison, BHV-1 gI contains one potential *N*-linked glycosylation site and eight potential *O*-linked glycosylation sites (Figure 1). In addition, a region immediately upstream of the transmembrane domain of BHV-5 gI, E_{247} to Q_{291} (Figure 1), show divergence from the predicted gI sequences for BHV-1. Comparison of predicted gI amino acid sequences between strain TX89 (this study) and Brazilian BHV-5 strain SV507/99 (Delhon *et al*, 2003) revealed only two amino acid differences, in the case of TX89 strain, A_{228} and T_{279} are replaced with T and A, respectively.

Construction and analysis of a BHV-5 gI-deleted (BHV-5 gIΔ) and BHV-5 gI-revertant (BHV-5 gIR) recombinant viruses

The DNA from BHV-5gIΔ enhanced green fluorescent protein (EGFP) and wild-type BHV-5 was analyzed by Southern blot hybridization to confirm the intended deletion of gI coding sequences. To ascertain that the phenotype of the deletion mutant was due solely to deletion of the gI gene, BHV-5 gI deletion was restored to wild type (BHV-5gIR) by DNA fragment spanning the gI-flanking and gI ORF–coding sequences (see Figure 8A). The presence of gI-coding

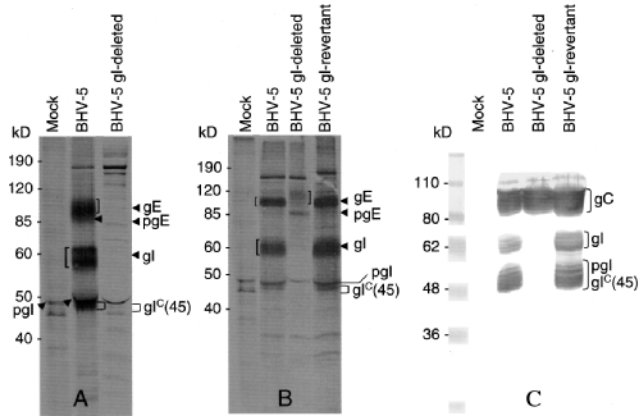

Figure 2 Characterization of gI-deleted and gI-reverted BHV-5 viruses by immunoprecipitation (**A** and **B**) and immunoblotting (**C**). For immunoprecipitation, mock- and virus-infected MDBK cells were labeled with [^{35}S]methionine-cysteine for 10 h. Detergent extracts were prepared and immunoprecipitated with (**A**) gI-specific and (**B**) gE-specific polyclonal rabbit antibody (Whitbeck *et al*, 1996). Mature gE (gE), mature gI (gI), precursor gE (pgE), and precursor gI (pgI) protein bands are marked. A 45-kDa proteolytic cleavage fragment (gI^C 45) of mature gI is indicated. Note that the mature gE expressed by the gI-deleted BHV-5 is a diffuse band with approximate molecular mass 94 to 100 kDa. (C) Immunoblotting analysis of BHV-5 wild-type, BHV-5 gI-deleted, and BHV-5 gI-revertant viruses. For immunoblotting, cocktail of gI-specific polyclonal rabbit antibody (Whitbeck *et al*, 1996) and BHV-5 gC-specific monoclonal antibody 8B1 (Chowdhury, 1995) was used. Note that in the gI-deleted BHV-5, gI-specific bands are lacking but the 94 to 96-kDa BHV-5 gC-specific band is present.

sequence in the wild-type BHV-5 but not in the BHV-5gIΔ EGFP indicated that the gI ORF–coding sequences have been deleted in the recombinant BHV-5gIΔ EGFP virus (data not shown). Consistent with this finding, 62-kDa, 46-kDa, and 45-kDa gI-specific bands (see below) were absent in the gI-deleted virus–infected cell lysates when immunoprecipiated or immunoblotted with anti-gI antibody (Figures 2A, C, respectively). However, the gI-specific antibody immunoprecipitated five proteins produced in BHV-5–infected cells (94-, 86-, 62-, 46-, and 45-kDa bands). The gE/gI homologs in alphaherpesviruses are coimmunoprecipitated with gE- and/or gI-specific serum (Montalvo *et al*, 1985; Whitbeck *et al*, 1996; Yao *et al*, 1993; Zuckermann *et al*, 1988). The 94-kDa and 86-kDa bands represent mature and precursor gE, respectively (Al-Mubarak *et al*, 2004; Chowdhury *et al*, 2000). The 62-kDa mature gI (gI), 46-kDa precursor gI (gI), and 45-kDa proteolytic cleavage product of the mature gI (gI^C 45) bands are gI-specific bands (see below). These bands were absent in the lysates of gI-deleted virus when immunoprecipitated with gI-specific antibody (Figure 2A). However, when immunoprecipiated with a gE-specific antibody (Figure 2B), only the gE precursor (86 kDa) and mature gE-specific diffused band (94 to 100 kDa) were precipitated from the infected cell lysates of gI-deleted BHV-5. These results confirmed that in BHV-5gIΔ virus, the gE gene is intact but was processed to a larger size protein (see below).

Growth properties and plaque size of BHV-5 gI-deleted virus in Madin-Darby bovin kidney (MDBK) cells

The growth properties and plaque size phenotypes of gI-deleted BHV-5, gE-deleted BHV-5, gI-reverted BHV-5, and wild-type BHV-5 were compared as described previously (Chowdhury *et al*, 2000). The gI- and gE-deleted BHV-5 grew with wild-type growth kinetics (data not shown). Both the gI- and gE-deleted BHV-5 viruses produced smaller plaques compared to wild-type; however, the gE-deleted virus produced smaller plaques when compared to that of gI-deleted BHV-5 (data not shown).

Synthesis and processing of gE/gI and gE in cells infected with BHV-5 wild-type and BHV-5gIΔ viruses

Immunoprecipitation and pulse-chase analysis of the wild-type BHV-5–infected cell proteins with gE-specific antibody show that gE/gI complex formation occured during the 30-min pulse (Figure 3). The dominant bands observed immediately after pulse (0-min sample) were the 86-kDa and 46-kDa forms of gE and gI, respectively. The 94-kDa mature gE and 62-kDa mature gI bands detected also at 0 time, as faint bands, were nearly equal by 30 min of chase to their respective 86-kDa (gE precursor) and 46-kDa (gI precursor) form. At the 120-min chase, the mature gE (94-kDa) and gI (62-kDa) bands became dominant, whereas the gE precursor (86-kDa) and gI precursor (46-kDa) bands diminished significantly. The

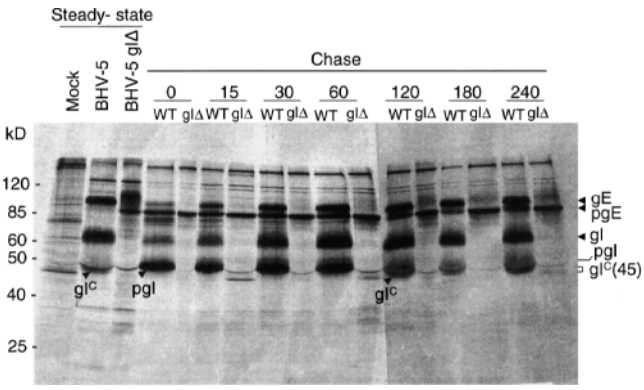

Figure 3 Autoradiograph showing pulse-chase analysis of gE in wild-type BHV-5 and in gI-deleted BHV-5-infected cell lysates. Infected MDBK cells were pulse-labeled for 30 min in 100 μCi of [^{35}S]cysteine and methionine per ml beginning at 6 h post infection. Cell monolayers were then washed twice with serum-free DMEM and were incubated in complete growth medium without labeled cysteine and methionine. Detergent extracts were prepared from identical samples harvested at times ranging from 0 to 240 min following the labeling period. Extract were then subjected to immunoprecipitation with gE-specific rabbit antiserum and analyzed by SDS-PAGE. Mock, BHV-5, and BHV-5 gIΔ (left most three lanes) represent cell lysates after steady-state labeling 10 h beginning at 6 h post infection.

86-kDa and 46-kDa gE and gI precursors, respectively, are processed in the endoplasmic reticulum (ER) and the 94-kDa and 62-kDa mature gE and gI, respectively are processed further within the Golgi (this study; Al-Mubarak *et al*, 2004). In addition, a diffuse band with an approximate molecular mass 45-kDa appeared by 120 min of chase (Figure 3). The 45-kDa band is a proteolytically cleaved product of the mature BHV-5 gI (Al-Mubarak *et al*, 2004).

To determine the synthesis and processing of gE in BHV-5 gI-deleted virus, similar pulse-chase and immunoprecipitation analysis with gE-specific antibody was performed and the results were compared with that of wild-type gE (Figure 3). At 0 time, only the 86-kDa ER-processed gE was detectable in the lysate of BHV-5 gI-deleted virus. The processed gE of the gI-deleted BHV-5 (94- to 100-kDa band) became detectable after a 120-min chase whereas the 94-kDa wild-type processed gE band became dominant at the 30-min chase. In the case of gI-deleted BHV-5, the amount of gE processed to its mature form was considerably reduced compared to the BHV-5 wild-type virus even after a 240-min chase (Figure 3). However, after steady-state 10 h of labeling, the amount of mature gE in the gI-deleted virus was increased considerably, though not up to the wild-type level. At this time, still a considerable amount of precursor gE was retained in the ER of the cells infected with the gI-deleted virus, whereas in the case of wild-type, gE precursor form was barely detectable (Figure 3). Interestingly, the molecular mass of the mature gE of BHV-5 gI-deleted virus produced a diffuse band ranging from 94 to 100 kDa (Figure 3). Therefore, the mature gE form of gI-deleted virus had heterogenous products with higher molecular mass. In addition, the maturation kinetics was delayed and the amount of mature gE was reduced relative to the wild-type virus.

Analysis of gE/gI processing in wild-type BHV-5–infected and gE processing in BHV-5gIΔ–infected cell lysates by glycopeptidase F(GlycoF) and endoglycosidase H (EndoH) treatment

The gE and gI precursors are predicted to acquire EndoH-sensitive, *N*-linked glycosylation in the ER, whereas the mature form of gE and gI (Golgi-modified) are predicted to contain EndoH-resistant, *N*-linked oligosaccharides. As a control, both the ER- and the Golgi apparatus–modified *N*-linked oligosaccharides can be removed by GlycoF. Maturation of gE in the gI-deleted virus was accompanied by a considerable increase in the apparent molecular mass. To test whether this was caused exclusively by modification of the *N*-linked glycans or due to additional processing in the Golgi, steady-state and 30-min pulse-chase–labeled BHV-5 wild-type– and BHV-5gIΔ–infected cell extracts were immunoprecipitated, as above, by gE-specific antibody. The immunoprecipitates were treated with EndoH (steady-state and 30-min pulse-chase samples) or with GlycoF (steady-state samples) as described in Materials and Methods. The results show that in the steady-state samples of wild-type and gI-deleted viruses, the 94-kDa and 94- to 100-kDa mature gE bands, respectively, were resistant to EndoH digestion (Figure 4A) but they were partially sensitive to GlycoF digestion (Figure 4B). The 86-kDa, ER-processed gE bands of wild-type and gI-deleted viruses were sensitive to both EndoH and GlycoF, resulting in slightly faster-migrating (approximately 1-kDa smaller) bands (Figure 4A, B). Therefore, the 94- to 100-kDa mature gE band of the gI-deleted BHV-5 was processed in the Golgi. Noticeably, a considerable amount of the 86-kDa EndoH-sensitive precursor gE of the gI-deleted virus was retained in the ER, whereas in the wild-type the precursor gE was barely detectable. In the 30-min pulse-chase samples of gI-deleted virus, mature gE (94- to 100-kDa) was also resistant to EndoH digestion, whereas the 86-kDa precursor gE was sensitive to EndoH digestion (Figure 4A). These results indicated that a proportion of the 86-kDa ER-processed gE of gI-deleted virus is transported to the Golgi and are processed further.

The results of GlycoF digestion also showed that the 94-kDa wild-type gE (Golgi-processed) and the 94- to 100-kDa gE band of gI-deleted BHV-5 (Golgi-processed) were not fully sensitive to GlycoF digestion and resulted in a 90-kDa (for wild-type gE) and diffused band with approximate molecular mass 90 to 94-kDa (for gI-deleted BHV-5) (Figure 4B). In the

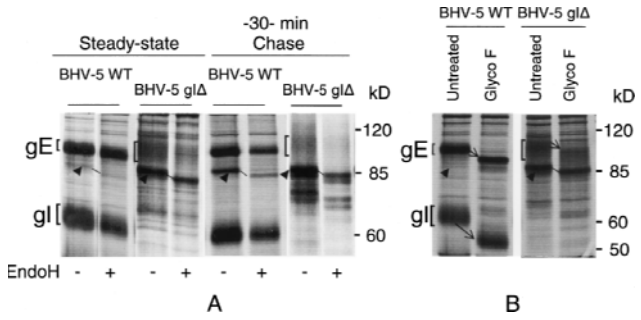

Figure 4 Endoglycosidase (Endo)H and glycopeptidase (Glyco)F digestion analysis of gE in BHV-5 and BHV-5 gI-deleted viruses. For EndoH digestion (**A**), infected MDBK cells were labeled steady-state or pulse-labeled for 30 min and chased for 30 min. Lysates of [^{35}S]methionine-cysteine–labeled cells were immunoprecipitated with gE-specific polyclonal rabbit serum and adjusted to 0.5% SDS. Samples were boiled for 10 min and digested with EndoH (+) as described in Materials and Methods. Samples were analyzed by SDS-PAGE (10% gel). For control, untreated samples (−) are shown. Mature ([) and precursor (►) gE expressed by wild-type and gI-deleted viruses are indicated. For GlycoF digestion (**B**), MDBK cells were labeled steady-state. Immunoprecipitated lysates were adjusted to 0.5%, boiled for 10 min, and digested with GlycoF as described in Materials and Methods. Samples were analyzed by SDS-PAGE (10% gel) as above. For control, untreaded samples are shown. Thin arrows indicate the shift in size of mature gE and gI bands after GlycoF digestion. Note that 94-kDa and 94- to 100-kDa mature gE bands of wild-type and gI-deleted viruses, respectively, are partially sensitive/resistant to GlycoF digestion.

GlycoF control, RNase B was fully sensitive to GlycoF (data not shown). The most likely interpretation of these results is that mature gE in wild-type and in gI-deleted BHV-5 acquired *O*-glycans in the Golgi or other post-translational modifications that are not altered by GlycoF. Therefore, the gE synthesized by gI-deleted virus is transport competent and was modified in the Golgi. However, it may have acquired heterogenous and/or additional post-translational modifications, resulting in a diffused band ranging from 94 to 100 kDa. Taken together the results of gE processing in the gI-deleted virus and the growth properties of gE- and gI-deleted viruses, it is concluded that even though the gE/gI interaction was necessary for the proper processing/glycosylation of the gE, this interaction is not important with respect to virus growth in tissue culture.

Surface expression of gE in wild-type and gI-deleted viruses

To confirm the results of pulse-chase and EndoH resistance of gE expressed in gI-deleted BHV-5, we then asked whether the processed gE reached the cell surface. Confocal microscopy images show that gE is expressed on the surface of BHV-5gIΔ–infected MDBK cells; however, the amount is less relative to the wild-type gE surface expression (Figure 5).

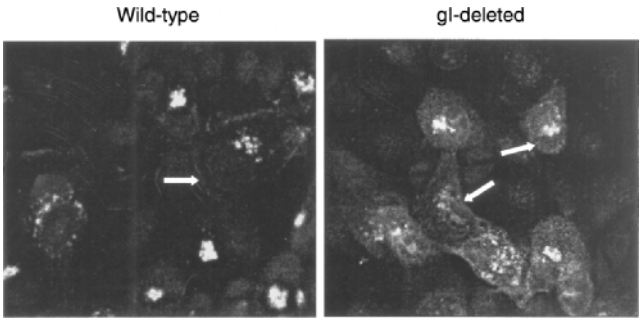

Figure 5 Surface expression of gE in cells infected with wild-type and gI-deleted BHV-5 viruses. MDBK cells were infected with wild-type (MOI of 5) and gI-deleted BHV-5 (MOI of 10). Fixed and permeabilized cells were reacted with rabbit anti gE polyclonal antibody and stained with Cy2- or Cy5-conjugated donkey anti-rabbit IgG for wild-type and gI-deleted BHV-5, respectively. Samples were examined with a BioRad MRC1024Es confocal laser scanning microscope. Confocal images were collected with a 60× objective using a 488-nm laser line for excitation and a 522-nm emission filter, with the phase-contrast mode of BioRad LaserSharp imaging program. Arrows point to surface labeling.

Pathogenicity of BHV-5 gI-deleted and BHV-5 gI-revertant viruses in rabbits

In the initial survival experiment, three out of six rabbits (50%) infected with BHV-5gIΔ had severe neurological signs (seizures) between 8 and 11 days post infection (dpi) and they were euthanized. The remaining three rabbits showed mild neurological signs and did not develop seizures. They were euthanized at 12 dpi. Their brains were processed for immunohistochemistry. In the second experiment, six rabbits were inoculated with gI-deleted BHV-5 and four rabbits were inoculated with BHV-5 gI-revertant (BHV-5 gIR). Two out of six rabbits (33%) infected with gI-deleted BHV-5 developed severe neurological signs by 10 dpi and two out of four rabbits (50%) infected with gI-revertant virus showed severe neurological signs by 10 dpi. All the rabbits were euthanized on 10 dpi or when the animals showed severe neurological signs. Brains were sectioned and processed for virus isolation as described earlier (Chowdhury *et al*, 1997). Virus isolation results are shown in Table 1. The amount of virus isolated from the rabbits infected with gI-deleted BHV-5 was slightly reduced when compared with the rabbits infected with gI-reverted BHV-5 (approximately similar amount from olfactory bulb, twofold less from anterior cortex and similar amount from posterior cortex). gI-deleted BHV-5 grew efficiently in the naso-olfactory mucosa and the amount of virus shed was comparable to that shed by rabbits infected with gI-reverted BHV-5 (Table 1). Statistical analysis (Microsoft Excel) of the number of rabbits showing severe neurological signs in the gI-deleted and gI-reverted groups did not reveal a significant difference ($P > .01$).

Spread of the gI-deleted BHV-5 in the CNS following intranasal infection was evaluated by immunostaining and compared with that of the

Table 1 Summary of clinical signs and virus isolation

Virus	*Animal no.*	*Neurological signs*[a]	*PFU,*[b] *nose, 3 dpi*	*Virus isolation*		
				Olfactory bulb	*Anterior cortex*	*Posterior cortex*
BHV-5gIΔ (expt. 1)	6	Severe (3)	ND[c]	ND[c]	ND[c]	ND[c]
BHV-5gIΔ (expt. 2)	6	Severe (2)	1.6×10^3	+[e](2)	++[d](3)	+++(4)
BHV-5gIR	4	Severe (2)	1.8×10^3	+[e](2)	++[e](3)	+++(4)

[a]Numbers in parenthesis indicate number of animals showing clinical signs or brain segments positive for virus isolation.
[b]Average PFU.
[c]ND, not determined.
[d]Mid range.
[e]Higher end.
1–190 PFU/g (+), 200–1990 PFU/g (++), >2000 PFU/g (+++).

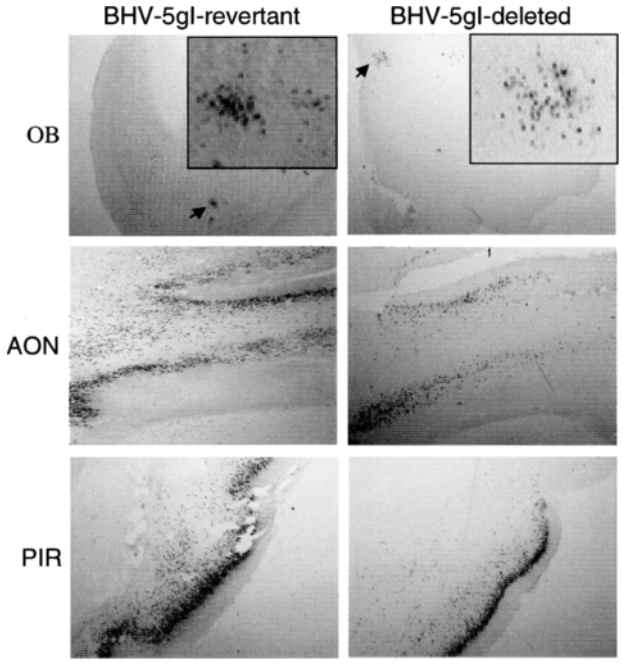

Figure 6 Localization of viral antigen in brain sections. Animals were inoculated intranasally with either gI–deleted or gI–revertant BHV-5 as described in Materials and Methods. The animals were euthanized on days 6, 8, and 10 days post infection or when they showed neurological signs. The brains were processed for immunohistochemical analysis as described in Materials and Methods. Representative sections of the olfactory bulb (OB), anterior olfactory nucleus (AON), and piriform cortex (PIR) are shown. Sections shown are form day 10 post infection. For OB, insets show magnified areas marked (→).

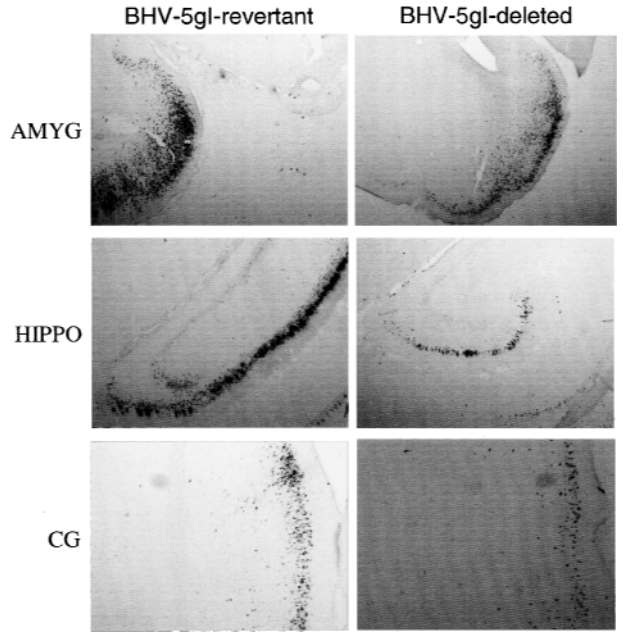

Figure 7 Localization of viral antigen in representative sections showing the amygdala (AMYG), hippocampus (HIPPO), and cingulate cortex (CG). Sections shown are from day 10 post infection.

Table 2 Summary of viral spread in the brain after intranasal inoculation

	Presence and location of viral antigen[a]					
Virus	*OB*	*AON*	*PIR*	*HIPPO*	*AMYG*	*CG*
BHV-5gIR	++[b]	++++[d]	++++[d]	++++[c]	++++[d]	+++[b]
BHV-5gIΔ	++[b]	++++[b]	++++[c]	+++[c]	++++[c]	++[c]

[a]Indicated as 1 to 25 (+), 30 to 150 (++), 160 to 500 (+++), or 550 to 3000 (++++) labeled neurons per field at a magnification of ×5.
[b]Lower end of the range.
[c]Mid range.
[d]Higher end of the range.
OB, olfactory bulb; AON, anterior olfactory nucleus; PIR, piriform cortex; HIPPO, hippocampus; AMYG, amygdala; CG, cingulate cortex. Scores for BHV-5gIR and wild-type are average of six rabbits and for each segment five sections were counted (30 slides for each section). Scores for BHV-5gIΔ are average of 10 rabbits and for each brain segment five sections (total 50 sections) were analyzed.

BHV-5 gI-revertant. Virus-specific antigens were detected in the olfactory bulb (second-order neurons) at 6 dpi. By 8 to 10 dpi, infected neurons were detected in the anterior olfactory nucleus (third-order neurons) and in piriform cortex, amygdala, hippocampus, and frontal and cingulate cortices (fourth and/or fifth order neurons). The number of neurons infected by gI-deleted BHV-5 were approximately similar (in olfactory bulb and piriform cortex), three- to fourfold less (in anterior olfactory nucleus and hippocampus), and twofold less (in amygdala and cingulate cortex) when compared with the gI-revertant virus (Figures 6, 7, Table 2). The gI-deleted virus spread to the hippocampus and cingulate cortex (fifth-order neuronal connection) but compared to the gI-revertant BHV-5, there were similar or two- to fourfold less number of infected neurons for the gI-deleted BHV-5. Taken together, these results show that the number of infected neurons for the gI-deleted virus was slightly lower but they were sufficient to produce severe neurological signs in 40% (50% in the first experiment and 33% in the second experiment) rabbits (Table 1).

Discussion

We conducted this study to determine the role of the gI gene in BHV-5 neuropathogenesis and neurovirulence using a rabbit seizure model. The BHV-5 gI sequence of an American strain (TX89) was determined and the predicted amino acid sequence of the gI was compared with those of BHV-1 gI and gI of a Brazilian BHV-5 strain. We generated a BHV-5 gI-deleted recombinant virus and investigated the neurovirulence and neuroinvasive properties of the gI-deleted and gI-revertant BHV-5 viruses in a rabbit seizure model (Chowdhury *et al*, 1997). The processing and maturation of gE in the gI-deleted virus was characterized and compared with that of the wild-type BHV-5. The studies demonstrated that gE

expressed by the gI-deleted BHV-5 is processed in the Golgi to a higher molecular mass protein and that the gI-deleted BHV-5 retained significant neurovirulence and neural spread within the brain.

The results of pulse-chase experiment showed that although the gE expressed by the wild-type virus is processed to a 94-kDa protein, mature gE of the gI-deleted virus is processed to a larger and diffused protein of 94- to 100-kDa molecular mass. In addition, the kinetics of gE maturation was delayed and the amount of mature gE was reduced in the gI-deleted virus. Even though with time a considerable amount of precursor gE of gI-deleted virus was transported to the Golgi and processed to its mature EndoH-resistant form, a noticeable amount of precursor gE was still detectable in the gI-deleted BHV-5 after 10 h of labeling, whereas in the wild-type, the precursor gE was barely detectable. These results suggested that, like in other alphaherpesviruses, including BHV-1, the export of gE from the ER to the Golgi is inefficient unless gI is present (Enquist *et al*, 1999; Mallory *et al*, 1997; Whitbeck *et al*, 1996; Yao *et al*, 1993). Consistent with this finding, a reduced amount of gE reached the cell surface in cells infected with gI-deleted BHV-5 when compared to wild-type BHV-5–infected cells. Both the gEs (expressed by wild-type and gI-deleted viruses) were partially sensitive to GlycoF digestion, which indicated that, like in other alphaherpesviruses, the gE might have acquired additional *O*-glycans in the Golgi (Cohen *et al*, 1997; Yao *et al*, 1993).

Noticeably, gE expressed in the gI-deleted BHV-5 attained a larger molecular mass. In BHV-1 and PRV, gE is also processed in the Golgi with a delayed kinetics when expressed without a gI, but it is not known to acquire a larger molecular mass (Whitbeck *et al*, 1996). In BHV-1, the first 246 amino acids of gE are important for the complex formation with the gI (Tyborowska *et al*, 2000) and in HSV-1, predicted amino acid residues 183 to 288 mediate complex formation with the gI (Basu *et al*, 1995). In BHV-5, the amino-terminal third of the gE is predicted to be important for the gE/gI complex formation (Al-Mubarak *et al*, 2004). Because the precursor gEs of wild-type and gI-deleted BHV-5 have identical molecular mass and the gE-gI complex is formed prior to the post-translational modifications in the Golgi (Al-Mubarak *et al*, 2004), the larger molecular mass of the mature gE expressed by the mutant virus is presumably due to additional glycosylation. It is possible that in the presence of gI, potential glycosylation sites present in the gE amino-terminal region, important for the complex formation, are not available within the Golgi for further processing, when the gE is complexed with the gI. But in the absence of gI, they become available for further processing, resulting, in a protein with a larger molecular mass. Indeed, predicted amino acid sequence analysis for potential glycosylation sites show that within the first 246 amino acids of BHV-5 gE, there are five potential *O*-glycosylation sites (S83, T220, T222, S226, T231) and one potential *N*-glycosylation sites (N150) (Chowdhury *et al*, 2000). The BHV-1 gE predicted amino acid sequence lacks the corresponding potential *O*-glycosylation sites (Chowdhury *et al*, 2000). Accordingly, BHV-1 gE, when expressed without the gI, is processed to its normal 92-kDa size but with a slower kinetics. Therefore, it is possible that in the absence of gI, additional *O*-glycosylation sites noted above for BHV-5 gE are accessible for further processing in the Golgi and acquire additional *O*-glycans, which could account for the larger BHV-5 gE when expressed without the gI. Similar phenomenon was also observed in the case of varicella-zoster virus (VZV) when gE was expressed alone either from a gE-expressing plasmid clone (Yao *et al*, 1993) or by a gI-deleted virus (Cohen *et al*, 1997), resulting in a slightly larger gE.

In rabbits, gI-deleted BHV-5 retains significant neurovirulence and its neural spread is identical to the gI-revertant BHV-5. In case of gI-deleted BHV-5, about 40% of rabbits show severe neurological signs, whereas for gI-reverted BHV-5, about 50% of rabbits show severe neurological signs. Virus recovered from the brains and nasal swabs also showed that the rabbits infected with BHV-5 gI-deleted virus yielded a very similar amount compared to the BHV-5 gI-revertant virus. Earlier, we have reported that 70% to 80% of rabbits infected with wild-type BHV-5 show severe neurological signs (Lee *et al*, 1999) and that rabbits infected with gE-deleted BHV-5 do not show severe neurological signs at all (Chowdhury *et al*, 2000). Unlike gI-deleted BHV-5, gE-deleted BHV-5 replication within the brains of infected rabbits was significantly reduced when compared with the gE-reverted BHV-5 (Chowdhury *et al*, 2000). The differences in the number of animals showing severe neurological signs when infected with the gI-deleted, gI-reverted, and wild-type BHV-5 were not statistically significant.

Based on the immunohistochemistry data, the gI-deleted BHV-5 virus invaded first-, second-, third-, and fourth-order neurons in the olfactory pathway. But fewer neurons (ranging from similar to fourfold less) were infected when compared with rabbits infected with the BHV-5 gI-revertant virus. However, in the case of gE-deleted BHV-5, the neural spread of the virus was reduced significantly (Chowdhury *et al*, 2000). Together, our data suggest that in the absence of gI, gE is sufficient to retain BHV-5 neurovirulence and neural spread. However, in the absence of gE, BHV-5 gI is not sufficient to retain the neurovirulence and neural spread of the virus (Chowdhury *et al*, 2000).

In PRV, both gE and gI deletion results in significant reduction in the neurovirulence of the virus (Husak *et al*, 2000; Kimman *et al*, 1992; Kritas *et al*, 1994, 1995; Whealy *et al*, 1993). Even though the gE-deleted PRV is more attenuated than the gI-deleted virus (Kritas *et al*, 1994, 1995), both in pigs and in a rat eye model, the gI-deleted PRV was attenuated

significantly when compared with the wild-type (Card and Enquist, 1995; Husak *et al*, 2000; Kritas *et al*, 1994, 1995). In contrast, the BHV-5 gI-deleted virus retains significant neurovirulence.

Like in other alphaherpesviruses, both the gE- (Chowdhury *et al*, 2000) and gI-deleted BHV-5 (this study) forms small plaque phenotype *in vitro* and the gI-deleted virus forms slightly larger plaques than that of gE-deleted BHV-5. However, unlike other alphaherpesviruses, neural spread and neurovirulence of the gI-deleted BHV-5 was indistinguishable from the wild-type BHV-5. This *in vivo* neurovirulent phenotype for the gI-deleted BHV-5 was unexpected and it does not fit to our current view on gE/gI functions in alphaherpesviruses and their interdependence both *in vitro* and *in vivo*. Therefore, one might question our results in light of gI's role *in vivo*. A PRV recombinant expressing BHV-1 gI alone spread anterogradely to visual centers in rats and does not require its obligate partner BHV-1 gE, but a PRV expressing BHV-1 gE did not show similar spread phenotype (Knapp *et al*, 1997). In this instance, gE and not the gI was dispensable *in vivo*, but it does clearly indicate that even though the gE/gI functions are conserved among the alphaherpesviruses, there are subtle differences between the alphaherpesviruses in their role *in vivo*.

In HSV-1, one of the suggested functions of gI was to modify HSV-1 gE in its affinity for binding to IgG (Johnson and Feenstra, 1987; Johnson *et al*, 1988). Fc receptor activity of PRV gE/gI (Favoreel *et al*, 1997) and VZV gE/gI (Litwin *et al*, 1992) has also been reported, but we and others were unable to show any Fc receptor activity of the BHV-1 and BHV-5 gE-gI complex (Chowdhury *et al*, 2000; Whitbeck *et al*, 1996). It is possible that gE-gI complex formation is necessary for the wild-type level gE processing; however, a small quantity of processed BHV-5 gE is sufficient for BHV-5 neural spread and neurovirulence in rabbits. Similarly in PRV, a small quantity of gE in the virus envelope was also sufficient for anterograde neural spread and neurovirulence (Tirabassi *et al*, 1997).

Based on a structural analysis of alphaherpesvirus gD, gG, and gI sequences, it has been proposed that gG and gI of alphaherpesviruses are related to gD and that they have been derived from a common ancestor (McGeoch, 1990). Therefore, in the absence of gI, another glycoprotein i.e., gD, may compensate for the neurovirulence and cell-to-cell spread function of gI *in vivo*. Even though this hypothesis has yet to be tested for BHV-5 and other alphaherpesviruses, it is possible that indeed there is an evolutionary relationship of these proteins.

Materials and methods

Virus strain and cell lines

BHV-5 TX89 strain (Chowdhury *et al*, 1997) was used in this study. The viruses were propagated and titrated in MDBK cells grown in Dulbecco modified Eagle's medium (DMEM) supplemented with heat-inactivated 10% fetal bovine serum.

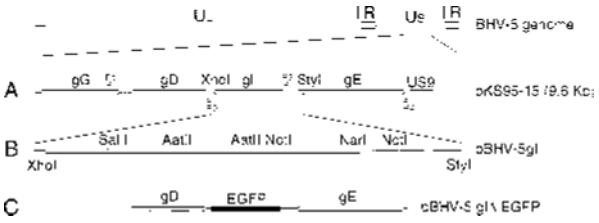

Figure 8 BHV-5 genomic structure and schematic map of gI deletion plasmid. The genomic organization of BHV-5 depicted at the top consists of unique long (U_L) and unique short (U_S) regions and two repeat regions (I_R and T_R). (**A**) Location of the gI and flanking genes. (**B**) A restriction site map of the1.58 kb XhoI and StyI fragment. (**C**) Genomic organization of the mutant pBHV-5gIΔ clone showing the replacement of the entire gI ORF with EGFP gene.

Cloning and sequencing of the BHV-5 gI gene

The authors have previously cloned the BHV-5 9.6-kb StuI/StuI fragment containing the region spanning from BHV-5 gG to Us9 and its 170-bp downstream sequences (pKS-95-15) (Figure 8). The nucleotide sequence of BHV-5 gD and gE genes, flanking the BHV-5 gI gene homolog, has been previously determined in the authors' laboratory (Abdelmagid *et al*, 1995; Chowdhury *et al*, 2000). The gI gene is located within the 1.58-kb XhoI/StyI subfragment of pKS95-15. To determine the gI gene coding sequence, we first cloned the 1.58-kb XhoI/StyI fragment into XhoI/XbaI sites of pGEM-7Z, resulting in plasmid clone pBHV-5gI. A restriction map of the cloned fragment was constructed, and subclones spanning the entire fragment were generated. The DNA sequence was determined by the Iowa State University sequencing facility.

Sequence analysis

The sequences obtained from subclones spanning the entire gI coding region were assembled using the seqaid II sequence analysis software as reported before (Chowdhury *et al*, 2000). The predicted amino acid sequences of BHV-5 gI and BHV-1 gI (Leung-Tack *et al*, 1994) were aligned using the GCG BestFit program (Genetic Computer Group) (gap weight, 8; length weight, 2). Hydropathicity analysis (Kyte and Doolittle, 1982) was performed using a 9–amino acid window. The prediction of signal sequence was determined using the Signal Prediction program from the World Wide Web (Signal Prediction, V2.0, http://www.cbs.dtu.dk/cgi-bin/nph) (Nielsen *et al*, 1997).

Construction of gI deletion plasmid

For the construction of the BHV-5gI deletion vector, the gI upstream and downstream flanking regions were generated by polymerase chain reaction (PCR). Using primer pairs P1 (CCCAGAATTCCGCCCGCTCCGAGCGCCGC), P2 (GCGCGGTACCTTTATCTCCC-

GCCC-CGCGCA),and P3 (GCGTGGATCCGTCTGTC-TCGGTTTCTGCGC), P4 (AGTTAAGCTTGACGACG-CTGTGTGGACTCTCC) and pKS95-15 DNA as a template, 1.9-kb and 2.15-kb fragments, respectively, were amplified. These primer pairs incorporated EcoRI-KpnI (P1 and P2, respectively) and BamHI-HindIII (P3 and P4, respectively) at the 5′ and 3′ ends of the respective amplified fragment (underlined sequences represent the restriction sites). After PCR amplification, the P1-P2 and P3-P4 products were digested with EcoRI-KpnI and BamHI-HindIII enzymes, respectively, and cloned into the EcoRI-KpnI and BamHI-HindIII sites of plasmid pGEM-3Z (Promega, Madison, WI). The resulting clone (pBHV-5gIΔ 5′3′) lacked the entire gI ORF, but it contained the gI upstream gD sequences and gI downstream gE-flanking sequences located immediately adjacent to the KpnI and BamHI sites, respectively. The pEGFP/C1 (Clontech Lab.) plasmid containing the EGFP gene cassette was modified by deleting sequences, spanning XhoI (blunt) to BamHI (blunt) sites, in the multiple cloning site, with resulting plasmid pEGFP/C1-collapse. To insert the EGFP gene cassette at the BamHI site of gI deletion vector, pBHV-5gIΔ 5′3′ was digested with BamHI, blunt ended, and a 1.7-kb AseI (blunt)/MluI (blunt) fragment (containing the entire GFP) from pEGFP/C1-collapse was inserted and religated. The resulting plasmid pBHV-5gI GFPΔ lacks the entire gI ORF and the GFP gene is flanked by the gI upstream and downstream sequences (Figure 8).

Generation of recombinant viruses

gI-deleted GFP-expressing BHV-5 (BHV-5gIΔ GFP): To generate a gI-deleted BHV-5 recombinant, full-length wild-type BHV-5 and linearized pBHV-5gIΔ GFP DNA was cotransfected into MDBK cells as described earlier (Chowdhury *et al*, 2000). Recombinant viruses expressing GFP were plaque purified by agar overlay and by identifying green fluorescence plaques under a fluorescent microscope. They were then further characterized by Southern blot (using gI ORF sequences as a probe) and by immunoblotting using gI-specific antibody (Whitbeck *et al*, 1996).

gI-revertant mutant of BHV-5 (BHV-5gIR): To determine the specificity of the gI deletion, BHV-5 gI-revertant virus was generated by cotransfection of full-length BHV-5gIΔGFP virus DNA and the linearized pKS95-15 DNA (containing the entire gI gene and its flanking gD and gE sequences) into MDBK cells. Nonfluorescent plaques were plaque purified and analyzed by Western blotting for wild-type gI expression.

Preparation of radiolabeled mock- and virus-infected cell lysates and immunoprecipitation

For steady-state labeling, confluent MDBK cells were infected with wild-type BHV-5 and recombinant BHV-5gIΔGFP, at multiplicity of infection (MOI) of 5 for 6 h prior to labeling with [^{35}S]methionine-cysteine. Mock infections with virus-free medium were always included in the analysis. Lysates were collected at 16 h post infection in extraction buffer (40% *w*/*v* suspension) as described earlier (Chowdhury *et al*, 2000). Immunoprecipitation and sodium dodecyl sulfate–polyacrylamide gel electrophoresis (SDS-PAGE) was performed as described previously (Chowdhury *et al*, 2000).

Pulse-chase analysis

Confluent MDBK cells were infected with wild-type BHV-5 and recombinant BHV-5gIΔGFP at MOI of 5 PFU per cell. At 4 h post infection, complete growth medium (DMEM, 5% fetal bovine serum) was replaced with serum- and cysteine-methionine–free medium (Sigma, St. Louis, Mo.). At 6 h postinfection, the medium was replaced with cysteine-methionine-free medium containing 1% serum, and 100μ Ci of [^{35}S]methionine-cysteine per milliliter. The infected cells were incubated at 37°C for 30 min. At the end of the labeling period, the cells were washed twice in prewarmed (37°C) serum-free medium and were either harvested immediately (0-min chase) or incubated at 37°C in complete growth medium for an additional 15 to 240 min. At the end of each of the chase periods, individual samples were processed as previously described (Chowdhury *et al*, 2000) and radioactively labeled infected cell lysates were immunoprecipitated with gE-specific antibody and analyzed by SDS-PAGE as described previously (Chowdhury *et al*, 2000).

GlycoF and EndoH digestion

The immunoprecipitated viral proteins were released from the Sepharose beads with immobilized protein A by boiling in 20 μl of 0.5% SDS and 1% β-mercaptoethanol for 10 min. The supernatants were transferred to fresh tubes. For GycoF digestion, the supernatants were adjusted to 50 mM sodium phosphate (pH 7.5), 1% NP-40, and incubated with 1000 U of GlycoF (New England Biolab) in a total volume of 26 μl for 1 h at 37°C. For EndoH digestion, the supernatants were adjusted to 50 mM sodium citrate (pH 5.5) and incubated with 100 U of EndoH (New England Biolab) in a total volume of 22.2 μl for 1 h at 37°C. The digested samples were subjected to SDS-PAGE and labeled proteins were visualized via autoradiography.

Western blot analysis

Cellular extracts and purified virion lysates were electrophoresed on a 10% SDS polyacrylamide gel and transferred to nitrocellulose membrane. Proteins were visualized by using rabbit polyclonal antibodies as described previously (Chowdhury *et al*, 2000).

Indirect immunofluorescence

MDBK cells grown on chamber slides were infected with gI-deleted or wild-type BHV-5. At 10 h post

infection, cells were fixed with 3.5% neutral buffered formaldehyde (20 min), permeabilized with 0.5% Igepal CA 630 (Sigma). After blocking with 5% horse serum in phosphate-buffered saline for 1 h at room temperature, they were then incubated for 2 to 3 h at room temperature with rabbit anti-gE-specific antibody, washed, and stained with Cy2- or Cy5-conjugated donkey anti-rabbit IgG (Jackson Immune Res), for wild-type and gI-deleted BHV-5, respectively. The slides were cover slipped with gel/mount (Biomeda Corp, Foster city, CA).

Animal experiments

Four-week-old New Zealand white rabbits weighing 500 to 600 g (Myrtles Rabbitry, Thomson Station, TN) were used. Rabbits were maintained in laboratory isolation cages in our vivarium throughout the experiments, with food and water freely available. All procedures were approved by the Kansas State University Animal Care and Use Committee.

A rabbit seizure model described previously (Chowdhury *et al*, 1997; Lee *et al*, 1999) was used to compare the neuropathogenic properties of gI-deleted and gI-reverted BHV-5 viruses. Unless otherwise mentioned, 2×10^7 PFU of virus were inoculated per nostril. Following infection, the rabbits were observed four times per day for the appearance of neurological symptoms. Nasal swabs were obtained on 3 dpi for virus isolation. For virus isolation from the brain, rabbits were euthanized at 10 dpi or when they showed severe neurological signs. Brains were sectioned and processed as described earlier (Chowdhury *et al*, 1997).

To compare the neural spreads of different viruses, rabbits were inoculated with each virus as described above. Rabbits were euthanized and perfused transcardially at 6, 8, 10, and 12 dpi for gI-deleted viruses. For gI-revertant viruses, rabbits were euthanized at 10 dpi or when they showed severe neurological signs. The brain was processed for immunohistochemistry as described earlier (Lee *et al*, 1999).

Nucleotide sequence accession number

The nucleotide sequence of the BHV-5 gI gene of TX89 strain has been submitted to GenBank, with accession number AY498717.

References

Abdelgamid OY, Minocha HC, Collins JK (1995). Fine mapping of bovine herpesvirus-1 (BHV-1) glycoprotein (gD) neutralizing epitopes by type-specific monoclonal antibodies and sequence comparison with BHV-5 gD. *Virology* **206:** 242–253.

Al-Mubarak A, Zhou Y, Chowdhury SI (2004). A glycine-rich BHV-5 gE-specific epitope within the ectodomain is important for BHV-5 neurovirulence. *J Virol* **78:** 4806–4816.

Ashbaugh SE, Thompson KE, Belknap EB, Schultheiss PC, Chowdhury SI, Collins JK (1997). Specific detection of shedding and latency of bovine herpesvirus 1 and 5 using a nested polymerase chain reaction. *J Vet Diag Invest* **9:** 387–394.

Basu S, Dubin G, Basu M, Nguyen V, Friedman HM (1995). Characterization of regions of herpes simplex virus type 1 glycoprotein E involved in binding the Fc domain of monomeric IgG and in forming a complex with glycoprotein I. *J Immunol* **154**: 260–267.

Belknap EB, Collins JK, Ayers VK, Schultheiss PC (1994). Experimental infection of neonatal calves with neurovirulent bovine herpesvirus type 1.3. *Vet Pathol* **31:** 358–365.

Brideau AD, Card JP, Enquist LW (2000). Role of pseudorabies virus Us9, a type II membrane protein, in infection of tissue culture cells and the rat nervous system. *J Virol* **74:** 834–845.

Card JP, Enquist LW (1995). Neurovirulence of pseudorabies virus.*Crit Rev Neurobiol* **9:** 137–162.

Card JP, Whealy ME, Robbins AK, Enquist LW (1992). Pseudorabies virus envelope glycoprotein gI influences both neurotropism and virulence during infection of the rat visual system. *J Virol* **66:** 3032–3041.

Chowdhury SI (1995). Molecular basis of antigenic variation between the glycoproteins C of respiratory bovine herpesvirus 1 (BHV-1) and neurovirulent BHV-5. *Virol* **213:** 558–568.

Chowdhury SI, Lee BJ, Mosier D, Sur J-H, Osorio FA, Kennedy G, Weiss ML (1997). Neuropathology of bovine herpesvirus type 5 (BHV-5) meningo-encephalitis in a rabbit seizure model. *J Comp Pathol* **117:** 295–310.

Chowdhury SI, Lee BJ, Ozkul A, Weiss ML (2000). Bovine herpesvirus 5 glycoprotein E is important for the neuroinvasiveness and neurovirulence in the olfactory pathway of the rabbit. *J Virol* **74:** 2094–2106.

Chowdhury SI, Onderci M, Bhattacharjee PS, Al-Mubarak A, Weiss ML, Zhou Y (2002). Bovine herpesvirus 5 (BHV-5) Us9 is essential for BHV-5 neuropathogenesis. *J Virol* **76:** 3839–3851.

Cohen JI, Nguyen H (1997). Varicella-zoster virus glycoprotein I is essential for growth of virus in vero cells. *J Virol* **71:** 6913–6920.

Delhon G, Moraes MP, Lu Z, Afonso CL, Flores EF, Weiblen R, Kutish GF, Rock DL (2003). Genome of bovine herpesvirus 5. *J Virol* **77:** 10339–10347.

Dingwell KS, Doering LC, Johnson DC (1995). Glycoproteins E and I facilitate neuron-to-neuron spread of herpes simplex virus. *J Virol* **69:** 7087–7098.

Dingwell KS, Johnson DC (1998). The herpes simplex virus gE-gI complex facilitates cell-to-cell spread and binds to components of cell junctions. *J Virol* **72:** 8933–8942.

D'Offay JM, Mock RE, Fulton RW (1993). Isolation and characterization of encephalitic bovine herpesvirus type 1 isolates from cattle in North America. *Am J Vet Res* **54:** 534–539.

Enquist LW, Husak PJ, Banfield BW, Smith GA (1999). Infection and spread of alpha herpesviruses in the nervous system. *Adv Virus Res* **51:** 237–347.

Favoreel HW, Nauwynck HJ, Van Oostveldt P, Mettenleiter TC, Pensaert MB (1997). Antibody-induced and cytoskeleton-mediated redistribution and shedding of viral glycoproteins, expressed on pseudorabies virus infected cells. *J Virol* **71:** 8254–8261.

Fehler F, Herrmann JM, Saalmuller A, Mettenleiter TC, Keil GM (1992). Glycoprotein IV of bovine herpesvirus 1-expressing cell line complements and rescues a conditionally lethal viral mutant. *J Virol* **66:** 831–839.

Husak PJ, Kuo T, Enquist LW (2000). Pseudorabies virus membrane proteins gI and gE facilitate anterograde spread of infection in projection-specific neurons in the rat. *J Virol* **74:** 10975–10983.

Johnson DC, Feenstra V (1987). Identification of a novel herpes simplex virus type1-induced glycoprotein which complexes with gE and binds immunoglobulin. *J Virol* **61:** 2208–2216.

Johnson DC, Frame MC, Ligas MW, Cross AM, Stow ND (1988). Herpes simplex virus immunoglobulin G Fc receptor activity depends on a complex of two viral glycoproteins, gE and gI. *J Virol* **62:** 1347–1354.

Kimman TG, de Wind N, Oei-Lie N, Pol JMA, Berns AJM, Gielkens ALJ (1992). Contribution of single genes within the unique short region of Aujeszky's disease virus (suid herpes type 1) to virulence, pathogenesis and immunogenicity. *J Gen Virol* **73:** 243–251.

Knapp AC, Husak PJ, Enquist LW (1997). The gE and gI homologs from two alphaherpesviruses have conserved and divergent neuroinvasive properties. *J Virol* **71:** 5820–5827.

Kritas SK, Nauwynck HJ, Pensaert MB (1995). Dissemination of wild-type and gC-, gE- and gI-deleted mutants of Aujeszky's disease virus in the maxillary nerve and trigeminal ganglion of pigs after intranasal inoculation. *J Gen Virol* **76:** 2063–2066.

Kritas SK, Pensaert MB, Mettenleiter TC (1994). Role of envelope glycoproteins gI, gp63 and gIII in the invasion and spread of Aujeszky's disease virus in the olfactory nervous pathway of the pig. *J Gen Virol* **75:** 2319–2327.

Kyte J, Doolittle RF (1982). A simple method for displaying the hydropathic character of a protein. *J Mol Biol* **157:** 105–132.

Lee BJ, Weiss ML, Mosier D, Chowdhury SI (1999). Spread of bovine herpesvirus type 5 (BHV-5) in the rabbit brain after intranasal inoculation. *J NeuroVirol* **5:** 474–484.

Leung-Tack P, Audonnet JC, Rivière M (1994). The complete DNA sequence and genetic organization of the short unique region (US) of the bovine herpes virus type 1 (ST strain). *Virology* **199:** 409–421.

Litwin V, Jackson W, Grose C (1992). Receptor properties of two varicella-zoster virus glycoproteins, gpI and gpIV, homologous to herpes simplex virus gE and gI. *J Virol* **66:** 3643–3651.

Mallory S, Sommer M, Arvin AM (1997). Mutational analysis of the role of glycoprotein I in varicella-zoster virus replication and its effects on glycoprotein E conformation and trafficking. *J Virol* **71:** 8279–8288.

McGeoch DJ (1990). Evolutionary relationships of virion glycoprotein genes in the S regions of alphaherpesvirus genomes. *J Gen Virol* **71:** 2361–2367.

Montalvo EA, Parmley RT, Grose C (1985). Structural analysis of the varicella-zoster virus gp98-gp62 complex: posttranslational addition of *N*-linked and *O*-linked oligosaccharide moieties. *J Virol* **53:** 761–770.

Mulder WAM, Jacobs L, Priem J, Kok GL, Wagenaar F, Kimman TG, Pol JMA (1994). Glycoprotein gE-negative pseudorabies virus has a reduced capability to infect second- and third-order neurons of the olfactory and trigeminal routes in the porcine central nervous system. *J Gen Virol* **75:** 3095–3106.

Nielsen H, Engelbrecht J, Brunak S, Heijne GV (1997). Identification of prokaryotic and eukaryotic signal peptides and prediction of their cleavage sites. *Protein Engin* **10:** 1–6.

Rock DL, Hagemoser WA, Osorio FA, Reed DE (1986). Detection of bovine herpesvirus type 1 RNA in trigeminal ganglia of latently infected rabbits by in situ hybridization. *J Gen Virol* **67:** 2515–2520.

Tirabassi RS, Townley RA, Eldridge MG, Enquist LW (1997). Characterization of pseudorabies virus mutants expressing carboxy-terminal truncations of gE: evidence for envelope incorporation, virulence, and neurotropism domains. *J Virol* **71:** 6455–6464.

Tyborowska J, Bienkowska-Szewczyk K, Rychlowski M, Van Oirschot JT, Rijsewijk FAM (2000). The extracellular part of glycoprotein E of bovine herpesvirus 1 is sufficient for complex formation with glycoprotein I but not for cell-to-cell spread. *Arch Virol* **145**: 333–351.

Whealy ME, Card JP, Robbins AK, Dubin JR, Rziha HJ, Enquist LW (1993). Specific pseudorabies virus infection of the rat visual system requires both gI and gp63 glycoproteins. *J Virol* **67:** 3786–3797.

Whitbeck JC, Knapp AC, Enquist LW, Lawrence WC, Bello LJ (1996). Synthesis, processing, and oligomerization of the bovine herpes virus 1 gE and gI membrane proteins. *J Virol* **70:** 7878–7884.

Wyler R, Engels M, Schwyzer M (1989). Infectious bovine rhinotracheitis/ vulvo-vaginitis (BHV-1). In: *Herpesvirus diseases of cattle, horses and pigs*. Wittman, G (ed). Hingham, MA: Kluwer Academic Publishers, pp 1–72.

Yao Z, Jackson W, Forghani B, Grose C (1993). Varicella-zoster virus glycoprotein gpI/gpIV receptor: expression, complex formation, and antigenicity within the vaccinia virus T7 RNA polymerase transfection system. *J Virol* **67:** 305–314.

Zuckermann FA, Mettenleiter TC, Schreurs C, Sugg N, Ben-Porat T (1988). Complex between glycoproteins gI and gp63 of pseudorabies virus: its effect on virus replication. *J Virol* **62:** 4622–4626.